PHYSICAL REVIEW B **80**, 060101(R) (2009)

Role of di-interstitial clusters in oxygen transport in UO_{2+x} from first principles

D. A. Andersson,[1] T. Watanabe,[2] C. Deo,[3] and B. P. Uberuaga[1]
[1]*Materials Science and Technology Division, Los Alamos National Laboratory, Los Alamos, New Mexico 87545, USA*
[2]*School of Chemical and Biomolecular Engineering, Georgia Institute of Technology, Atlanta, Georgia 30332, USA*
[3]*Nuclear and Radiological Engineering Program, George W. Woodruff School of Mechanical Engineering, Georgia Institute of Technology, Atlanta, Georgia 30332, USA*
(Received 1 July 2009; published 10 August 2009)

Using density functional theory, we examine a recently discovered structure for di-interstitial oxygen clusters in UO_{2+x} in which three oxygen ions share one lattice site. This di-interstitial cluster exhibits a fast diffusion pathway; the migration barrier for these clusters is approximately half of that for mono-interstitials. Using kinetic Monte Carlo, we calculate the diffusivity of oxygen with and without the di-interstitial mechanism as a function of x and find that oxygen transport is significantly increased for higher values of x when the di-interstitial mechanism is included, agreeing much more closely with experimental data. These results emphasize the importance of clustering phenomena in UO_{2+x} and have implications for the evolution of UO_{2+x}.

DOI: 10.1103/PhysRevB.80.060101 PACS number(s): 61.72.Bb, 66.30.Dn, 66.30.H−

Urania, UO_2, is the primary component of fuels in many nuclear reactors and under operating conditions or after fabrication often exists in hyperstoichiometric form, UO_{2+x}. In UO_{2+x}, oxygen ions occupy interstitial or interstitial-like sites in the parent fluorite lattice (CaF_2 type) and U^{5+} or U^{6+} ions act as charge-compensating defects. The thermodynamic and kinetic properties of the excess oxygen ions govern radiation tolerance, fission product accommodation, fission gas release and micro-structural evolution.[1]

Depending on stoichiometry and temperature, UO_{2+x} can phase separate into UO_2 and U_4O_9.[2,3] In this Rapide Communication, we focus on the high-temperature regime where UO_{2+x} forms a solid solution and the excess oxygen can be viewed as interstitials in the UO_2 structure. In the simplest model of UO_{2+x}, these interstitials are assumed to randomly occupy the empty octahedral interstitial positions in the fluorite lattice. For increasing nonstoichiometry (larger x), however, the oxygen ions are known to aggregate.[4,5] Propositions for the structure of these clusters include the so-called 2:2:2 Willis cluster[4,5] and the cuboctahedral cluster.[6] Recent theoretical work identified new geometries for clusters of oxygen interstitials in UO_{2+x}, encompassing both di-interstitials[8,9] and quadinterstitials.[8]

Experimental studies of oxygen diffusion in UO_{2+x} for low x have found that the activation energy for oxygen diffusion ranges from 0.9 to 1.3 eV,[10–15] with 0.9–1.0 eV identified as the most probable regime.[13] Diffusion in the low x regime is typically ascribed to the motion of already-present oxygen interstitials. The diffusivity initially increases as function of x and then saturates, and even decreases, for high x.

In this Rapid Communication we employ density functional theory (DFT) based methods to explore the stability of oxygen interstitial clusters in UO_{2+x}, as well as the corresponding migration paths and barriers. The kinetic parameters thus obtained are then used in a kinetic Monte Carlo (kMC) model to study oxygen transport as a function of composition in UO_{2+x}.

The DFT calculations were performed with the Vienna *ab initio* simulation package (VASP) (Refs. 16–18) using the projector augmented wave (PAW) method.[19,20] The exchange and correlation effects were treated within both the generalized gradient approximation (GGA) (Ref. 21) and the local density approximation with an additional onsite Hubbard U term included (LDA+U).[22] In agreement with earlier studies,[23–25] our GGA calculations predict UO_2 to be metallic and underestimate the lattice constant by 0.13 Å [5.34 Å compared to the experimental value of 5.47 Å (Ref. 26)]. The LDA+U method has been used in several studies[8,27–33] to describe the strongly correlated U-5f electrons more accurately and this methodology captures the correct Mott-insulating behavior of UO_2 as well as reproduces the experimental lattice constant ($\approx$5.45 Å). The LDA+U approach applied here was described in Ref. 8 and its predictions agree well with recent hybrid DFT treatments of strong correlations in UO_2.[34,35] Unless otherwise stated all reported numbers refer to the LDA+U calculations. Since test calculations showed that spin-polarized GGA calculations only provide a minor correction to the nonspin-polarized results for oxygen based defects,[36] the GGA calculations were performed at the nonspin-polarized level. A 2^3 supercell expansion of the cubic fluorite unit cell was used to study defect properties and the volume was held constant at the calculated volume of UO_2. All calculations used a 2^3 Monkhorst-Pack k-point mesh and the plane-wave cutoff was set to 400 eV. All internal structural parameters were relaxed until the Hellmann-Feynman forces on each ion were sufficiently small ($<$0.02 eV/Å).

Oxygen monointerstitials (I_1) in UO_{2+x} migrate by the interstitialcy mechanism. At large x, di-interstitial clusters are likely to be more abundant and, as we show here, exhibit a different diffusion mechanism. The diffusion pathways of mono-interstitials and di-interstitials were investigated with DFT-based dimer[37] and nudged elastic band[38] techniques. Due to the relative complexity of LDA+U we have only used these methods with GGA; thus, all barriers are calculated with GGA.

The migration rates of defects are expected to follow the Arrhenius relation for a thermally activated process: $k = \nu \exp(-E_m/k_bT)$, where k is the rate, E_m the migration barrier, ν the pre-exponential or attempt frequency factor, T is the temperature, and k_b is the Boltzmann constant. Using E_m

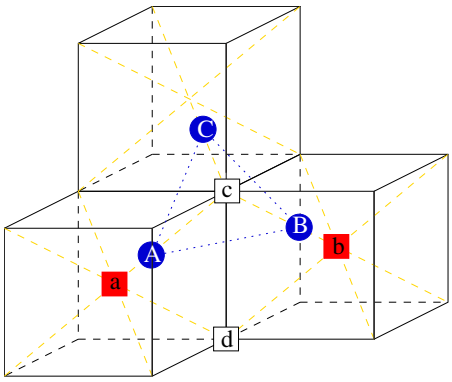

FIG. 1. (Color online) Idealized schematics of the structure of the I_2^O (red/solid squares) and I_2^X (blue/circles) di-interstitial structures. The cubes represent the simple-cubic oxygen sublattice; for clarity, U ions are not shown. The I_2^O structure has two oxygen interstitials (a and b) in octahedral interstitial sites in the lattice, while the remaining oxygen (c and d shown explicitly) remain in more or less perfect lattice sites. In the I_2^X structure, interstitial ions a and b move toward c to form the A-B-C structure, in which three oxygen ions share the one site originally occupied by ion c. Equivalently, a and b can push out d to form I_2^X. This motion of A-B-C to A-B-D via a-b is also the pathway discussed in the text for di-interstitial migration.

found from DFT, we constructed a kMC (Refs. 39–41) model of oxygen diffusion in UO_{2+x}. In all cases, interstitial oxygen atoms were distributed on a 40^3 unit cell lattice of the fluorite structure. We then calculate the mean square displacement (MSD) of individual oxygen and extract the diffusivity via the Einstein relation. The total diffusivity is then obtained as $D=\frac{x}{2+x}\langle D_i\rangle$, where $\langle D_i\rangle$ represents the averaged diffusivity of the individual oxygen ions and x the UO_{2+x} stoichiometry.

The point defect structures that have been analyzed in the present work include monointerstitials and di-interstitials of various types. Willis and co-workers[4,5] proposed a di-interstitial structure with two interstitial ions situated on octahedral sites with a very specific distortion of the surrounding oxygen ions. These distortions were so large that Willis and co-workers[4,5] described the resulting structure as a 2:2:2 cluster, comprised of, in essence, four interstitials and two vacancies. Starting from this structure and relaxing, we find this precise atomic arrangement to be unstable. In fact, it relaxes to one of two alternative structures. In what follows, we will thus consider only these two structures, hereafter referred to as the di-interstitial (I_2^O) and the split di-interstitial (I_2^X); the 2:2:2 cluster specifically proposed by Willis[4,5] is not considered further.

The di-interstitial I_2^O is composed of two oxygen interstitials residing in nearest neighbor octahedral sites (hence the superscript O in the label). We,[8] and others,[7,9,42] also found a structure, the split di-interstitial I_2^X, which consists of three oxygen ions arranged in an equiaxed (GGA) or equilateral (LDA+U) triangle centered on a vacant regular oxygen site and oriented on a {111} plane (the X label is inspired by notation often used to describe split mono-interstitials). Schematic illustrations of these two defect structures are shown in Fig. 1 and the bond geometries are defined in Table I.

We have calculated the relative stability of I_2^O versus I_2^X using both GGA and LDA+U. For each, we have performed two sets of calculations, corresponding to the GGA and LDA+U lattice constant, respectively, where the latter is close to the experimental value. The results are summarized in Table I. First, at the LDA+U experimental lattice constant, I_2^X is predicted to be the more stable di-interstitial cluster, being about 0.25 eV lower in energy than I_2^O. Using LDA+U at the GGA lattice constant, which corresponds to a pressure of 15 GPa, the stability difference is reduced to 0.04 eV. Interestingly, these trends are reproduced using the GGA functional. We thus conclude that the defect stability is not overly sensitive to the particular functional used, but rather the volume of the simulation cell. According to our calculations, the binding energy of monointerstitials to form di-interstitial clusters is negative or repulsive (−0.38 eV). Consequently, there is a net energetic driving force for dissociation; however this energy is small enough to allow a non-negligable fraction of di-interstitials to form at finite temperature, especially away from the dilute-limit stoichiometry range.

Using the dimer method at the LDA+U lattice constant, we have found a surprisingly fast diffusion mechanism for I_2, illustrated in Fig. 1. It actually involves both I_2^O and I_2^X. Starting from I_2^X (A-B-C), there is a barrier of 0.47 eV with GGA (but at the experimental lattice constant) for the structure to convert into I_2^O (a-b-c). There are three equivalent pathways for this motion, with the formation of I_2^O structures composed of the ions A and B (the I_2^O structure illustrated in Fig. 1), A and C, or B and C. I_2^O acts as an intermediate state and the a-b structure can transform into a second I_2^X structure by

TABLE I. The relative stability of I_2^X and I_2^O clusters [$\Delta E=E(I_2^O)-E(I_2^X)$], as well as the barrier associated with transforming the stable defect structure to the less stable structure (E_a). Data are reported for two different lattice constants (a_0) and for each a_0 both GGA and LDA+U numbers have been calculated. We use the notation XY to denote the distance between ion X and Y in Fig. 1, where X and Y represent A, B, C, a, b, or c. E_{xc} identifies the exchange-correlation functional used.

a_0 (Å)	E_{xc}	ΔE (eV)	E_a (eV)	AB (Å)	AC (Å)	CB (Å)	ab (Å)	ac (Å)	cb (Å)
5.45	LDA+U	0.25	n/a	2.75	2.64	2.64	3.56	2.43	2.47
5.45	GGA	0.31	0.47	2.57	2.57	2.58	3.35	2.39	2.40
5.34	LDA+U	0.04	n/a	2.79	2.69	2.69	3.60	2.41	2.43
5.34	GGA	0.03	0.40	2.59	2.60	2.60	3.44	2.39	2.34

kicking out d or return to the previous state by kicking out c. The barrier to move from I_2^O to I_2^X is 0.16 eV. There are four equivalent pathways for $I_2^O \rightarrow I_2^X$ motion (a and b can kick out either c or d, and each of those can move into one of two positions). Thus, the net barrier for I_2 diffusion at the experimental lattice constant is 0.47 eV. This is relatively fast, especially compared to the migration barrier of I_1:0.81 eV, again at the experimental lattice constant. Thus, in a situation in which a large number of interstitials are present (large x), and di-interstitials form via random encounters of I_1, a new fast diffusion pathway exists for oxygen transport. For comparison, at the GGA lattice constant, the migration barriers are 1.22 eV for I_1 and 0.40 eV for I_2. A recent study by Ichinomiya *et al.*,[42] using temperature accelerated dynamics (TAD),[43] also find a fast diffusion pathway for I_2, though the details differ.

In the kMC simulations, we consider two cases. In the first case, only mono-interstitials can move, and they can only move into an interstitial site if that site is empty. Mono-interstitials are also prevented from occupying nearest neighbor sites. This blocking model is motivated by the repulsion between oxygen interstitials occupying nearest-neighbor octahedral sites[8] and it is the same as used by Murch.[12] However, in reality this repulsion is not infinite, as assumed by this model, and the repulsion may be reduced by forming the more complex I_2^X di-interstitial defect configurations. In the second kMC case we model these modified interactions by allowing di-interstitial clusters to form and provide a second diffusion mechanism that could change the diffusion behavior. In the second model di-interstitials may form with a rate governed by the calculated binding energy and I_1 diffusion barrier, and then hop via the faster di-interstitial mechanism. Clusters containing more than two interstitial are prevented from forming via a blocking scheme equivalent to the one used for mono-interstitials in the first kMC model; that is this model is as simple an extension of the first model as possible and still allows for the formation of I_2. The effective barrier for dissolving a di-interstitial is 0.43 eV, which is slightly lower than the I_2^X migration barrier of 0.47 eV. The dissolution barrier results from assuming diffusion-limited formation of the initial di-interstitial. In both models, we used $\nu = 1 \times 10^{12}$, which also gives good agreement with experiments at low x. The oxygen interstitial diffusivities (D) for these two models are plotted as a function of the non-stoichiometry (x) in Fig. 2 and compared with the experimental observations.[10,11] All simulations and observations are at the same temperature, 1073 K. In the kMC model, we do not explicitly account for the I_2^X structure; for simplicity, we keep the interstitials on octahedral sites.

In the monointerstitial model, as x increases, D initially increases until the interstitials begin to interact with each other by blocking available diffusion paths, which results in decreasing D for high x. It is seen that the oxygen diffusivity calculated by this simple blocking model is in good agreement with experimental observations at low x but is much lower than the maximum D at $x \approx 0.12$. The inclusion of the di-interstitial mechanism increases the oxygen diffusivity at all non-stoichiometric values, but the effect is more pronounced at higher x values. The oxygen diffusivity is much closer to the experimental results when di-interstitial diffusion is incorporated into the kMC model. This is a combined effect of less restrictive blocking due to formation of the more stable I_2^X clusters and the fact that these clusters may migrate with a barrier that is close to the cluster disassociation barrier. For low x, where the influence of di-interstitials should be small, the diffusivity is almost indistinguishable from the monointerstitial mechanism. Simulations where mono-interstitials do not block nearest-neighbor sites give rise to a diffusivity that increases much too fast as function of x (not shown). Even within the di-interstitial model the simulated data exhibits a slightly sharper downturn than experiments, which could be related to formation of even larger clusters at high x.[8] This would imply less restrictive blocking than for the current di-interstitial kMC model, which, in accordance with difference between the two present models based on I_1 and I_2, may increase the diffusivity at high x.

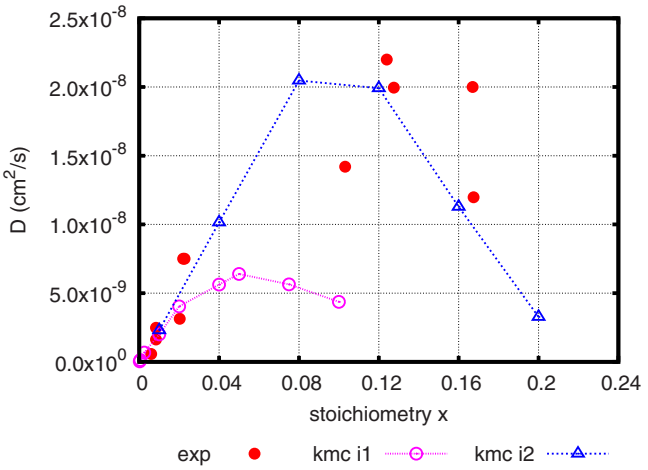

FIG. 2. (Color online) Oxygen diffusivity as a function of non-stoichiometry at 1073 K. The open blue triangles ('kmc i2') are the results of the simulation that take into account the di-interstitial motion, the open pink circles ('kmc i1') represent the simulation results from the simple blocking model and the red circles ('exp') represent the experimental observations of Marin and Contamin (Ref. 10) and Contamin *et al.* (Ref. 11).

To summarize, we have examined a recently discovered di-interstitial structure, referred to here as a split di-interstitial, which is energetically competitive with structures previously described in the literature. Furthermore, we have found a fast diffusion mechanism for di-interstitials that incorporates the split di-interstitial structure. This di-interstitial and its diffusion pathway account for the fast oxygen transport seen experimentally at intermediate x. This emphasizes the importance of cluster formation in UO_{2+x} and extends the significance of split di-interstitials from thermodynamic to the kinetic properties. We also speculate that similar diffusion mechanisms may be found in other fluorite derived materials and, if the di-interstitial clusters could be stabilized by, e.g., chemical alterations, such materials could provide very high ionic conductivity.

Work at Los Alamos National Laboratory was funded by DOE Nuclear Energy Fuel Cycle Research and Development (FCRD) Campaign, Nuclear Energy Advanced Modeling and Simulation (NEAMS) Program, Fuels Integrated Perfor-

mance and Safety Code (IPSC) project under the AFCI Modeling and Simulation work package No. LA0915090108 as well as OBES Division of Chemical Sciences under Contract No. W-7405. D.A.A. also acknowledges support from the Seaborg Instituite at Los Alamos National Laboratory. Los Alamos National Laboratory is operated by Los Alamos National Security, LLC, for the National Nuclear Security Administration of the U.S. DOE under Contract No. DE-AC52–06NA25396. C.D. was supported by DOE NERI-C (Grant No. DEFG07–14891).

[1] M. Stan and P. Cristea, Trans. Am. Nucl. Soc. **91**, 491 (2004).
[2] B. T. M. Willis, J. Chem. Soc., Faraday Trans. 2 **83**, 1073 (1987).
[3] S. D. Conradson, D. Manara, F. Wastin, D. L. Clark, G. H. Lander, L. A. Morales, J. Rebizant, and V. V. Rondinella, Inorg. Chem. **43**, 6922 (2004).
[4] B. T. M. Willis, Acta Crystallogr., Sect. A: Cryst. Phys., Diffr., Theor. Gen. Crystallogr. **34**, 88 (1978).
[5] B. T. M. Willis, Nature (London) **197**, 755 (1963).
[6] D. J. M. Bevan, I. E. Grey, and B. T. M. Willis, J. Solid State Chem. **61**, 1 (1986).
[7] H. Y. Geng, Y. Chen, Y. Kaneta, and M. Kinoshita, Appl. Phys. Lett. **93**, 201903 (2008).
[8] D. A. Andersson, J. Lezama, B. P. Uberuaga, C. Deo, and S. D. Conradson, Phys. Rev. B **79**, 024110 (2009).
[9] K. Govers, S. Lemehov, M. Hou, and M. Verwerft, J. Nucl. Mater. **366**, 161 (2007).
[10] J. F. Marin and P. Contamin, J. Nucl. Mater. **30**, 16 (1969).
[11] P. Contamin, J. J. Bacmann, and J. F. Marin, J. Nucl. Mater. **42**, 54 (1972).
[12] G. E. Murch, D. H. Bradhurst, and H. J. De Bruin, Philos. Mag. **32**, 1141 (1975).
[13] G. E. Murch, J. Chem. Soc., Faraday Trans. 2 **83**, 1157 (1987).
[14] H. Matzke, J. Chem. Soc., Faraday Trans. 2 **83**, 1121 (1987).
[15] J. Belle, J. Nucl. Mater. **30**, 3 (1969).
[16] G. Kresse and J. Hafner, Phys. Rev. B **48**, 13115 (1993).
[17] G. Kresse and J. Furthmüller, Comput. Mater. Sci. **6**, 15 (1996).
[18] G. Kresse and J. Furthmüller, Phys. Rev. B **54**, 11169 (1996).
[19] G. Kresse and D. Joubert, Phys. Rev. B **59**, 1758 (1999).
[20] P. E. Blöchl, Phys. Rev. B **50**, 17953 (1994).
[21] J. P. Perdew, J. A. Chevary, S. H. Vosko, K. A. Jackson, M. R. Pederson, D. J. Singh, and C. Fiolhais, Phys. Rev. B **46**, 6671 (1992).
[22] A. I. Liechtenstein, V. I. Anisimov, and J. Zaanen, Phys. Rev. B **52**, R5467 (1995).
[23] J. P. Crocombette, F. Jollet, T. N. Le, and T. Petit, Phys. Rev. B **64**, 104107 (2001).
[24] M. Freyss, T. Petit, and J.-P. Crocombette, J. Nucl. Mater. **347**, 44 (2005).
[25] P. A. Korzhavyi, L. Vitos, D. A. Andersson, and B. Johansson, Nature Mater. **3**, 225 (2004).
[26] M. Idiri, T. Le Bihan, S. Heathman, and J. Rebizant, Phys. Rev. B **70**, 014113 (2004).
[27] M. Iwasawa *et al.*, Mater. Trans. **47**, 2651 (2006).
[28] R. Laskowski, G. K. H. Madsen, P. Blaha, and K. Schwarz, Phys. Rev. B **69**, 140408(R) (2004).
[29] F. Gupta, G. Brillant, and A. Pasturel, Philos. Mag. **87**, 2561 (2007).
[30] H. Y. Geng, Y. Chen, Y. Kaneta, and M. Kinoshita, Phys. Rev. B **75**, 054111 (2007).
[31] H. Y. Geng, Y. Chen, Y. Kaneta, M. Iwasawa, T. Ohnuma, and M. Kinoshita, Phys. Rev. B **77**, 104120 (2008).
[32] P. Nerikar, T. Watanabe, J. S. Tulenko, S. R. Phillpot, and S. B. Sinnott, J. Nucl. Mater. **384**, 61 (2009).
[33] S. L. Dudarev, D. N. Manh, and A. P. Sutton, Philos. Mag. B **75**, 613 (1997).
[34] K. N. Kudin, G. E. Scuseria, and R. L. Martin, Phys. Rev. Lett. **89**, 266402 (2002).
[35] I. D. Prodan, G. E. Scuseria, and R. L. Martin, Phys. Rev. B **73**, 045104 (2006).
[36] M. Stan *et al.*, J. Alloys Compd. **444-445**, 415 (2007).
[37] G. Henkelman and H. Jonsson, J. Chem. Phys. **111**, 7010 (1999).
[38] G. Henkelman, B. P. Uberuaga, and H. Jonsson, J. Chem. Phys. **113**, 9901 (2000).
[39] A. B. Bortz, M. H. Kalos, and J. L. Lebowitz, J. Comput. Phys. **17**, 10 (1975).
[40] K. A. Fichthorn and W. H. Weinberg, J. Chem. Phys. **95**, 1090 (1991).
[41] A. F. Voter, in *Radiation Effects in Solids*, edited by K. E. Sickafus, E. A. Kotomin, and B. P. Uberuaga (Springer, NATO Publishing Unit, Dordrecht, The Netherlands, 2006), pp. 1–24.
[42] T. Ichinomiya, B. P. Uberuaga, K. E. Sickafus, Y. Nishiura, M. Itakura, Y. Chen, Y. Kaneta, and M. Kinoshita, J. Nucl. Mater. **384**, 315 (2009).
[43] M. R. Sørensen and A. F. Voter, J. Chem. Phys. **112**, 9599 (2000).